

Compressibility, kinetics, and phase transition in pressurized amorphous silicaKostya Trachenko^{1,2} and Martin T. Dove¹¹*Department of Earth Sciences, University of Cambridge, Downing Street, Cambridge, CB2 3EQ, United Kingdom*²*Cavendish Laboratories, University of Cambridge, Madingley Road, Cambridge, CB3 0HE, United Kingdom*

(Received 26 July 2002; revised manuscript received 23 October 2002; published 27 February 2003)

We model the process of densification of silica glass using molecular dynamics simulation in order to resolve the current controversy regarding the existence of the first-order phase transition in this material. We propose the picture in which the structural changes start to take place in the pressure window between 3 and 5 GPa, after which significant modifications take place with the structural breakdown in the medium range. We also study microscopic processes behind temperature-induced volume decrease of pressurized glass, seen experimentally. We simulate this process and observe similar negative thermal swelling, accompanied by considerable rebonding and relaxations processes. Global nature of rebonding, resulting from the extended character of floppy modes present in silica glass, yields a large value of temperature-induced densification. The densified structure shows broadening of the rings distribution, and we identify the microscopical changes that lead to the breakdown of the medium-range structure. The interesting observation from the long annealing of pressurized glass is the large-amplitude cooperative flow of atoms, which takes place as the structure relaxes through continuous rebonding and relaxation events.

DOI: 10.1103/PhysRevB.67.064107

PACS number(s): 61.43.-j, 62.50.+p, 91.60.Gf

I. INTRODUCTION

Detailed understanding of the densification process and structural changes in amorphous solids under pressure is appealing for both experimental and simulation work. One of the interesting questions that has been addressed recently is the nature of the phase transformation between low and high density amorphous phases. Remarkably, different glasses show different behavior under pressure. Amorphous ice shows sharp first-order phase transition.¹ There are also indications of the first-order transition between low- and high-density amorphous Si and Ge.²⁻⁴ On the other hand, transitions to a denser phase in amorphous SiO₂,⁵⁻¹⁹ GeO₂,^{5,17} and GeSe₂ (see Ref. 20, and references therein) are gradual and continuous. Computer simulations are often employed to interpret the experimental data and to understand the transition between low and high density phases and their structure. While for some amorphous materials simulations confirm experimental first-order phase transitions, including the transition pressures,⁴ and gradual transformations for others,²⁰ the picture for silica glass remains controversial.

When compressed beyond 20 GPa, silica glass becomes irreversible on decompression, showing about 20% increase in density.^{6,8,9} The pressure-induced transition into the densified phase has been the subject of a number of other experimental studies.^{5-9,15,17} No indication of a pressure-induced first-order phase transition behavior was experimentally found. Structural changes take place gradually under pressure.^{7,13} Decrease of volume on pressure occurs gradually as well, with no sharp change in volume reduction.^{15,17,19} In Ref. 17 it was particularly emphasized that densification in silica glass should not be viewed as the first-order phase transition. Finally, previous atomistic simulations of pressure effects addressed structural changes caused by pressure, but have not revealed a first-order-type behavior.^{9-11,14,16,18,21}

On the other hand, on the basis of a thermodynamic

analysis of the pressurized glass it was suggested that there must exist a first-order phase transition around 3 GPa.²² It was argued that the transition is kinetically hindered, but could be seen experimentally at high temperature. This point was later questioned in the literature,^{23,24} but was followed by an experiment that reported a 20% discontinuous decrease of volume of the glass structure pressurized to 3.6 GPa at 700 K.²⁵ This was attributed to the first-order phase transition predicted in Ref. 22. However, in the recent *in situ* experiments, the amount of temperature-induced densification was found to be about 7–8%.^{26,27}

In this paper we contribute to the debate about the existence of the first-order phase transition in silica glass, by providing the insights into the kinetics of structural changes in the pressurized structure. We perform molecular-dynamics (MD) simulations of the pressure effects in silica glass, in order to try to propose a noncontradictory picture of densification that is supported by both experiments and simulations. We start with noting that pressurized glass structure is at the state of nonequilibrium that gives rise to continuous rebonding events on the fast time scale.¹⁸ The pressurized glass structure appears to be constantly adjusting to external pressure by local rebonding events, which is accompanied by a continuous volume decrease, consistent with experimental observations.¹⁷ We then note that the thermodynamic analysis of densification suggesting the existence of a first-order transition²² is related to the existence of a pressure threshold of about 3 GPa that separates tetrahedral and nontetrahedral structure, but does not mark a true first-order phase transition that separates distinct equilibrium phases.

By analyzing the ability of compressed glass to support floppy modes [modes that do not require distortions of SiO₄ tetrahedra or rigid unit modes (RUM's)], we propose that structural changes start to develop in the pressure window between 3 and 5 GPa. In this window the structure densifies by RUM-type distortions, with only small amount of rebonding in the structure. After about 5 GPa the densification ne-

cessitates rebonding and modifications in the medium range of the structure, seen experimentally as the compressibility anomaly.^{17,19}

We note that the reversibility window in chalcogenide glasses has been found, which is located between the rigid and floppy state of glass.²⁸ The understanding of this phenomenon is believed to be important, since similar physical processes are related to the properties of high-temperature superconductors²⁹ and protein folding.³⁰ This work demonstrates that silica glass joins the class of amorphous materials that show the change of physical properties in the floppy-rigid window.

We simulate the *in situ* experiments which show temperature-induced densification of glass under pressure.^{25–27} We observe the volume decrease as temperature increases, which is accompanied by global processes of rebonding and relaxation processes. We suggest that densification seen in Refs. 25–27 is the result of fast kinetics of rebonding processes that take place globally in the tetrahedral (or nearly tetrahedral) structure. This originates from the flexibility of tetrahedral silica glass against floppy modes, which are extended vibrations in the glass structure. The analysis of the densified quenched structure shows broadening of the rings distribution and we identify the microscopic processes that accompany the breakdown of the medium-range structure. Finally, we comment on the difference between pressure-induced transitions in monoatomic and diatomic amorphous solids.

II. SIMULATION DETAILS

We used the code DL_POLY,³¹ which has been optimized for use on parallel computers. The starting atomic configurations of silica glass were obtained from the configurations of amorphous silicon formed by the Wooten-Weaire algorithm.³² Oxygen atoms were inserted along each Si-Si bond, and the structures were then relaxed in the simulations. These structures were used previously to study double-well potentials and floppy modes in silica glass,^{18,21,33–35} and we showed that the radial distribution functions (RDF's) of the relaxed structures and the calculated neutron scattering function are in excellent agreement with experimental data.³⁴

Our simulations were performed using configurations containing 512 and 4096 SiO₄ tetrahedra with periodic boundary conditions. We used the interatomic potential of Tsuneyuki *et al.*³⁶ of the form

$$V(r) = \frac{q_1 q_2}{4\pi\epsilon r} - \frac{C}{r^6} + B \exp(-r/\rho). \quad (1)$$

This model uses standard potential functions which have been parameterized using quantum-mechanical calculations on small clusters. It has been shown that the model is able to reproduce high-pressure silica polymorphs, as well as phase transitions at external pressure.^{36,37} Recently simulation studies employed this potential,^{16,22,38} as well as the similar van Beest potential,¹⁰ to address pressure effects in silica glass. The Tsuneyuki potential has been shown to accurately handle

structural changes that occur under pressure^{36,37,22,38} (see also Ref. 16, and references therein).

We performed simulations aimed at achieving equilibration during compression and decompression in stages using constant pressure/temperature (NPT) ensembles. For calculating vibrational densities, constant energy (NVE) ensembles were used. The pressure effects have been simulated at different temperatures, and the structures have been equilibrated at their respective temperatures before applying pressure. Similarly, thermal effects have been studied at different pressures, and we have equilibrated the structures at respective pressures before applying temperature. Initial equilibration have been performed for typically 20 ps in order to arrive at a target pressure. To then study the evolution of pressurized structures, we have performed long annealing for up to 25 ns.

III. ON THE FIRST-ORDER PHASE TRANSITION IN SILICA GLASS UNDER PRESSURE

A. Nonequilibrium state of pressurized glass: rebonding events and relaxation

Recently, we have performed MD simulations in order to understand the mechanism of densification in silica glass.¹⁸ We found that as pressure increases beyond 3 GPa and causes an increase of the average coordination numbers, patches of the glass structure become locally unstable, with atomic relaxations occurring in the form of large-amplitude atomic displacements. Unlike at zero pressure where large reorientations of SiO₄ units occur within tetrahedral topology, and are related to the existence of the two-level systems in glass,^{33–35} relaxations at elevated pressure necessarily involve rebonding.¹⁸ Rebonding events accompany the breakdown in the medium range structure at high pressure. We have called these events “coordinons” since they are accompanied by the transfer of the coordination numbers.¹⁸ We have shown that fast rebonding and subsequent relaxation processes are responsible for the irreversible densification of silica glass.¹⁸ Recently, a very similar conclusion has also been drawn from *in situ* experimental studies of pressurized silica.¹⁹

The important point from our previous study for the present work is that pressurized silica glass is in the nonequilibrium state. Uncompressed glass is already out of equilibrium with respect to the long range order of the crystalline phase, but here by nonequilibrium we mean local instabilities relative to a given topology of the pressurized structure that give rise to relaxation processes in the form of rebonding events. From our picture it follows that the potential energy landscape of a pressurized glass is partitioned into the minima with the difference of energies involved in rebonding events. Rebonding events result in the system moving to a lower minimum, and we have observed that 2 eV was the energy change in a typical rebonding event.¹⁸ The barrier between the minima is low enough to be overcome even at room temperature, as is seen experimentally as continuous relaxation.¹⁷

The natural consequence of the nonequilibrium state of pressurized glass is the continuous relaxation accompanied

by the volume decrease. This is confirmed by the experiment, in which a logarithmic decrease of volume is seen in SiO_2 and GeO_2 glasses at various values of pressure.¹⁷ In our previous simulation work we have observed a volume decrease as the glass proceeded to relax through rebonding and relaxation events towards a densified structure.¹⁸ This has enabled us to suggest that rebonding processes observed in the simulation provide the microscopic mechanism for the continuous relaxation observed experimentally. The existence of rebonding and relaxation processes originating from the nonequilibrium state of the pressurized glass will be used and discussed in the rest of the paper.

B. Thermodynamic analysis of pressure-induced densification

As mentioned above, it has been proposed, basing on the thermodynamic analysis at zero temperature, that a first-order phase transition exists in silica glass at about 3 GPa, which could be observed if the temperature is high enough to overcome the activation barrier.²² In this section we extend the thermodynamic analysis to higher temperatures and discuss the structural changes take place in the range between 3 and 5 GPa and their effect on the free energy curves.

We first note that the atomistic simulations of pressure-induced transition in crystalline materials (both MD and *ab initio*), overestimate the value of transition pressure, i.e., the pressure at which the volume changes discontinuously. On the other hand, thermodynamic analysis that is based on the equality of Gibbs free energies $G = U + PV - TS$ of two phases at transition pressure, gives the value, consistent with the experiment (see, for example, Refs. 4,39). In order to resolve this controversy, it has been suggested that the activation barrier exists along a specific reaction path in the simulation which suppresses the transition. In the experiment, any lattice defects would reduce or nullify this barrier. Of course, the thermodynamic analysis does not specify any reaction path, and is therefore expected to give a correct transition pressure.³⁹ Thus, complimentary to the analysis of calculated volume versus pressure, the thermodynamical analysis is employed to derive the correct value of transition pressure.

In principle, the thermodynamic analysis of a pressure-induced phase transition need not be limited to crystalline materials, and can be applied to glasses. It is important, however, that there exist two distinct states of amorphous solid (with normal and increased density) that are separated by the transition, and which are at equilibrium at respective pressures. In this case, analysis based on the equality of Gibbs energies at the transition point at compression and decompression shows the true first-order phase transition. For example, in the case of the pressure-induced transition in amorphous silicon, the first-order phase transition is seen experimentally, with a discontinuous volume change at around 10 GPa. This value of the transition pressure is reproduced in the simulation by calculating the Gibbs free energies at zero temperature.⁴ Both low and high density phases appear to be at equilibrium at respective pressures.

Unlike in amorphous silicon, no discontinuous volume change on pressure is seen in experiments or simulations of

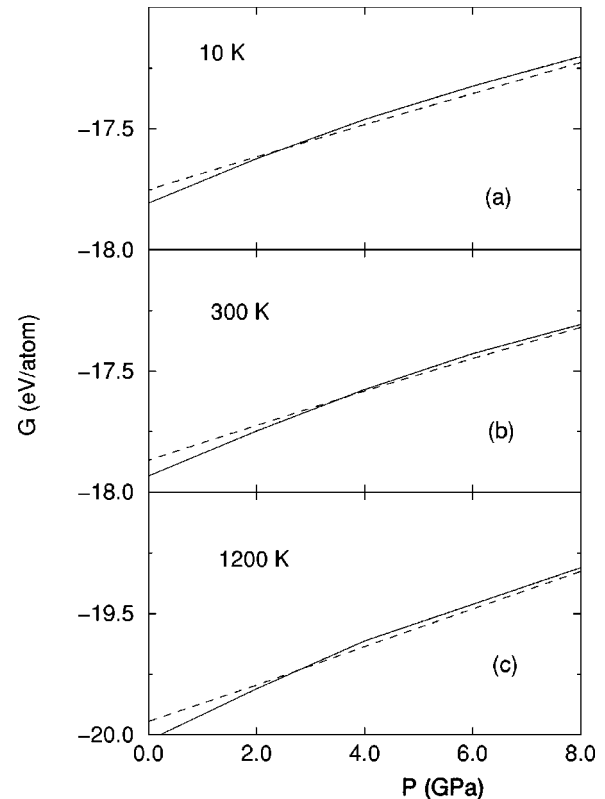


FIG. 1. Gibbs free energy as a function of pressure on compression (solid line) and decompression (dashed line) at 10 K (a), 300 K (b), and 1200 K (c).

silica glass: it transforms gradually to a more densified phase.⁵⁻¹⁹ Basing on experimental results, authors of Ref. 17 emphasized that the pressure-induced transformation should not be viewed as ordinary first-order transition.¹⁷ However, from calculating the free energies of silica glass structures on compression and decompression at zero temperature, it was suggested that the first-order phase transition should exist around 3 GPa.²² It was suggested that the transition is kinetically hindered and hence has not been observed yet, but can be seen if the temperature is high enough.²² In the simulation, we have not observed any indication of transition at around 3 GPa at very high temperatures up to the melting point. To understand the origin of possible transition better, we turn to the thermodynamical analysis.

We have compressed silica glass structures in stages of 2 GPa up to 20 GPa, and have calculated the Gibbs free energy at different temperatures on both compression and decompression. At high temperature, the last term in G becomes important, and one needs to calculate the contribution of vibrational entropy. In order to get the values of vibrational entropy, we have calculated velocity-velocity correlation function of structures on both compression and decompression. Vibrational densities of states were derived as the Fourier transforms of the correlation functions. Finally, the values of vibrational entropy were calculated from the vibrational densities of states (see, for example, Ref. 40) for each value of pressure on compression and decompression.

At different temperatures, the corresponding curves cross in the range 2–4 GPa, as can be seen in Fig. 1. This takes

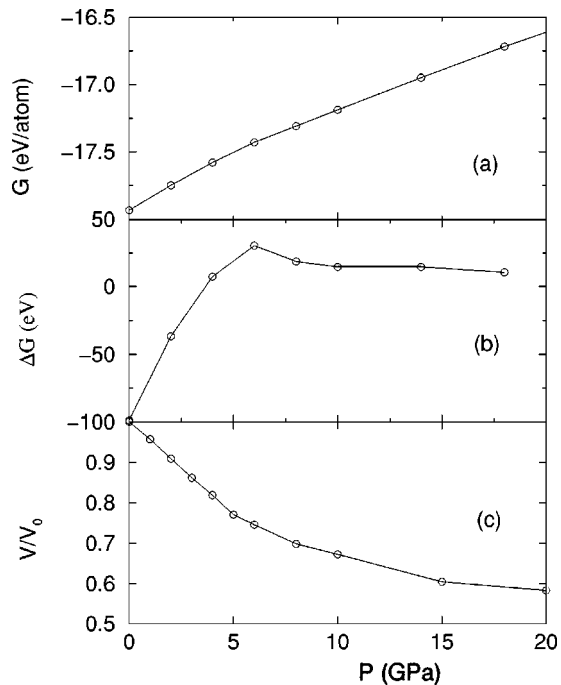


FIG. 2. Gibbs free energy on compression (a), difference between the Gibbs free energy on compression and decompression (b), and normalized volume (c) as a function of pressure. All results are taken at 300 K.

place as the slope of the Gibbs free energy on compression starts to develop a kink after about 5 GPa, while on decompression the free energy is essentially linear. Such a behavior originates from the fact that there is a threshold pressure (around 3 GPa) after which the increased coordinations start to appear in the structure.^{16,18,21} This is accompanied by rebonding and relaxation processes described in the previous section. Local rearrangements of the structure and relaxations to a densified state put the system's Gibbs free energy on the different slope. On the other hand, the structure is homogenous on decompression in a sense that it retains the high-pressure defects throughout the decompression process, up to complete pressure removal.¹⁸ Hence no kink develops in the free energy on decompression, resulting in crossing of compression and decompression curves to the left of the kink (between 2 and 4 GPa in Fig. 1).

It is interesting to note that the kink in the free energy coincides (within the computational error) which a change in slope of the volume decrease at about 5 GPa (see Fig. 1). This kink is particularly well seen in ΔG , the difference between Gibbs free energies on compression and decompression [Fig. 2(b)]. While 3 GPa is the threshold between tetrahedral and defective (nonideal) structure, 5 GPa marks the point at which a breakdown of the medium-range structure takes place, causing the kink in compressibility.

In the next sections we address the origin of the kink at 5 GPa, but we note here that the thermodynamic analysis presented above, as well as the one given in Ref. 22, does not imply the existence of the first-order phase transition around 3 GPa. There are no two distinct equilibrium phases that are separated by a possible first-order transition. Each value of

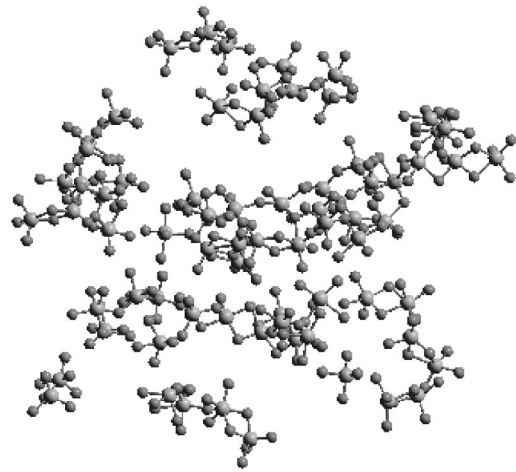


FIG. 3. Networks of connected SiO_4 polyhedra that have Si atoms bonded to more than four O atoms. The structure is pressurized to 6 GPa at 300 K.

pressure and temperature in Fig. 1 corresponds to a topologically distinct structure with a different number of “densification centers” (including increased local coordinations and broadening of the distribution of rings, as will be discussed below). Moreover, the number and structure of the densification centers (as well as the structure of normal density adjacent to the high density centers, see Ref. 18) constantly changes during rebonding and relaxation processes, and is the result of the nonequilibrium state of pressurized glass, as discussed in the previous section. Instead of the first-order transition at 3 GPa, we will propose the picture in which the transition to a more compact phase takes place gradually in the floppiness-rigidity window between about 3 and 5 GPa.

C. “Interaction” between densification centers

We note that pressure-induced transitions between amorphous phases of silica glass and ice have been studied in the simple model.²⁴ It has been shown that the gradual transformation takes place in the system if the interaction between constituent particles is weak, while global instability (first-order transition) occurs if the interaction is strong enough. In the former case, the mechanical instabilities are local and uncorrelated, and were linked to the absence of the first-order phase transition in silica glass. This was opposed to the case where strong interaction between particles triggers global instability, similar to the pressure-induced transformation in amorphous ice.²⁴

We find that parts of the densified silica glass may contain a connected network of polyhedra that have Si atoms with increased O coordinations (see Fig. 3). Higher pressure leads to the increase in the number of connected overcoordinated Si atoms. In the language of Ref. 24, there exists a certain “interaction” between the densification centers in our model, but it is not strong enough to trigger the first-order transition.

It is interesting to note in this context that a phase separation between the patches of normal and increased density has been reported in the simulation of liquid silica.⁴¹ This can be compared to the connected networks of densified cen-

ters seen in Fig. 3. The distinction should be drawn, however, between the essentially nonequilibrium states of pressurized silica glass, as discussed in the previous section, and the enhanced equilibration in the liquid silica. The latter considerably promotes the phase separation.⁴¹

IV. WINDOW IN THE PRESSURE-INDUCED DENSIFICATION

A. Structural changes and rebonding efficiency

We find that after 3 GPa structural changes start to take place in the form of rebonding and relaxation events. To estimate the degree of rebonding, we set up the list of neighbor O atoms to which a Si atom is bonded at each pressure, both on compression and decompression. This allows us to directly compare two structures, which we denote as A and B in terms of the number of broken and new bonds. If an O atom from the neighbor list of a given Si atom from structure A is not on the list of the corresponding Si atom in structure B, then one Si-O bond is counted as broken. Similarly, if an O atom from the neighbor list of a given Si atom from structure B is not on the corresponding Si list in structure A, then one Si-O bond is counted as new. On compression, we compare the initial structure at zero pressure (structure A) with the structure at elevated pressure P (structure B) and calculate the number of new and broken bonds as described above. We introduce the rebonding efficiency f , which is the ratio of the number of new bonds to the total number of bonds in the initial structure at zero pressure (the latter being equal to four times the number of Si atoms in the structure). This means that at a given pressure, the average number of Si-O bonds for each Si atom changes by $4f$.

We plot the dependence of volume on pressure at 300 K, together with the fraction of fourfold coordinated Si atoms and the number of new and broken bonds, in Fig. 4. First, the volume decreases linearly with pressure up to about 5 GPa, and changes its slope after this pressure [see Fig. 4(a)]. From Fig. 4(b) follows that the number of increased coordinations has two distinct regimes: the structure is compressible without the need to break the tetrahedral topology up to about 3 GPa: only fourfold Si coordinations are present in the structure and no rebonding takes place before 3 GPa. As the pressure increases beyond 3 GPa, further deformation of the network necessarily involves the appearance of increased coordinations. Finally, we find from Fig. 4(c) that rebonding starts to take place after 3 GPa, but increases its slope significantly at 5 GPa. All results are taken at 300 K.

Figure 4 shows that there is a pressure window between about 3 and 5 GPa, in which structural changes start to take place but become significant only beyond the window after 5 GPa. This is reflected in the experiments as the change of the slope of volume decrease at pressures exceeding 5 GPa.^{17,19} The origin of the pressure window will be addressed below.

B. Floppy modes in ideal and pressurized silica glass

We have found earlier that ideal silica glass structure supports floppy modes, motions that do not involve distortions of SiO₄ tetrahedra.⁴² This originates from the fact the num-

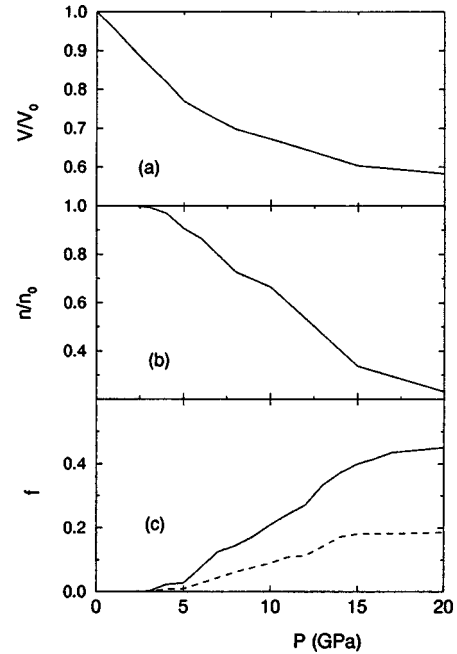


FIG. 4. Normalized volume (a), the number of fourfold coordinated Si atoms (b), and the number of new (solid line) and broken (dashed line) bonds as a function of pressure (c).

ber of constraints is equal to the number of degrees of freedom in the ideal tetrahedral network.^{33,34} Floppy, or rigid unit modes (RUM's) are seen in the neutron scattering experiments in silica glass as a broad band in the zero frequency range.³⁴ We have studied the effect of pressure on floppy modes and found that RUM's persist in silica glass structure up to about 3 GPa, the point up to which the structure is tetrahedral.²¹ After 3 GPa, Si atoms with increased coordinations start to appear, imposing more local constraints in the structure, which gradually loses the flexibility against RUM distortions. After about 5 GPa the structure becomes essentially stiff against floppy modes.²¹

The important point is that although 3 GPa divides the structure into tetrahedral and defective (nonideal), RUM-type distortions can persist in the structure until somewhat higher pressure of 5 GPa.²¹ We have verified this in more detail here by calculating RUM density of states for a number of pressures between 3 and 5 GPa, shown in Fig. 5. In our approach, the structure is RUM floppy, if RUM density of states is nonzero at zero frequency (see Refs. 33,34,21 for the description of the RUM model and formalism). Conversely, if RUM density of states is zero at zero frequency, the structure does not support RUM's.^{33,34,21} In the intermediate region the value of the density of states at zero frequency serves as the degree of RUM floppiness. As can be seen in Fig. 5, the structure gradually loses its ability to support RUM's in the range 3–5 GPa.

That the structure retains its RUM floppiness between 3 and 5 GPa has the following implication for the behavior of glass under pressure. Until 3 GPa, glass distorts by essentially RUM-type motion, i.e., without distortion of SiO₄ tetrahedra. To prove this, we have compared the ideal structure with the ones pressurized to 1, 2, and 3 GPa, using recently

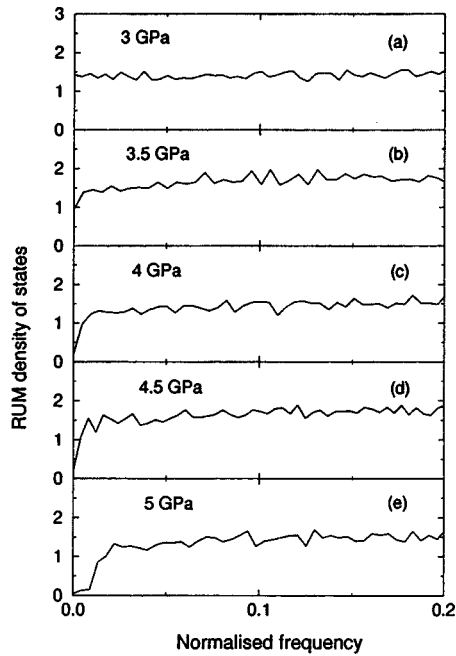


FIG. 5. Normalized RUM density of states of glass structure at 3 GPa (a), 3.5 GPa (b), 4 GPa (c), 4.5 GPa (d), and 5 GPa (e). Number of RUM's is given by the value of density of states at the origin. The decrease of the density of states at the origin on pressure increase can be seen in (a)–(d).

developed misfit method that is based on the geometric algebra operations.⁴³ We have found that the only distortions involved are RUM-type distortions. Between 3 and 5 GPa the structure becomes more rigid, but yet floppy enough to allow further structural modifications without causing the breakdown in the middle range. The result is that the volume and free energy continue to change linearly up to 5 GPa.

5 GPa marks the point at which large structural modifications necessarily accompany any further volume decrease. This is seen in the increased rate of rebonding events at 5 GPa in Fig. 4. Structural modifications are also reflected in the volume change as a kink in the volume change at 5 GPa and change in the slope of free energy (see Fig. 2).

The change of the response of structure to pressure exceeding 5 GPa is confirmed experimentally as a change of slope in the volume-pressure dependence.^{17,19} This is particularly well seen in the softening of the bulk modulus (compressibility anomaly) after about 5 GPa.¹⁹ From our analysis we attribute this change to the onset of large structural modifications in the medium range. In fact, our model also explains the increase of compressibility between about 3 and 5 GPa:^{17,19} as the number of RUM's decreases between 3 and 5 GPa, the structure stiffens up, since there are less ways to distort at low energy cost.

C. Reversibility window

We have seen that as pressure decreases the number of RUMs in the window between 3 and 5 GPa, the structure is still able to use the remaining portion of them to distort without causing rebonding in the structure. This means that

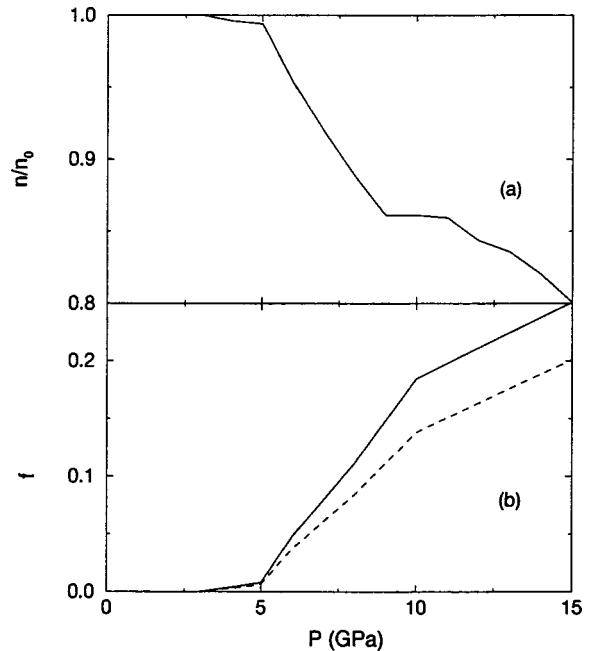


FIG. 6. Fraction of fourfold-coordinated Si atoms in decompressed structures (a) and the number of new and broken bonds calculated by comparing initial and decompressed structures (b) as a function of pressure P . All results are taken at 300 K.

the pressure-induced transformation in this window is essentially reversible, since it is rebonding and subsequent relaxations that yield the irreversible changes in the structure on decompression.¹⁸ We prove this point by calculating the fraction of fourfold-coordinated Si atoms in the structures decompressed from pressure P as a function of pressure, together with the number of new and broken bonds calculated by comparing the initial and decompressed structures (see Fig. 6).

We find that although some slight irreversibility is present between 3 and 5 GPa, corresponding to the beginning of rebonding process, the structure is able to use the remaining RUM's to distort without a considerable structural modifications. It is only at 5 GPa when the structure becomes stiff against RUM distortions, large irreversible changes start to take place. This is seen as the substantial increase in the irreversibility of both coordination numbers and rebonding degree at 5 GPa seen in Fig. 6.

It is interesting to note that the reversibility window has been found in chalcogenide glass $\text{Si}_x\text{Se}_{1-x}$.²⁸ This window has been shown to be located between rigid and floppy state of glass, which is tuned by x . The understanding of this effect is believed to be important since similar mechanism can be behind the properties of high temperature superconductors²⁹ and protein folding.³⁰ It appears that different disordered materials can assume similar reversibility windows that originate between the floppy state and rigid state of the structure. In the present model the transition from floppy to rigid is controlled by pressure, i.e., pressure can serve as a floppy-rigid tuning parameter that is similar to chemical composition x .²⁸ The details of pressure window in silica glass will be discussed elsewhere.

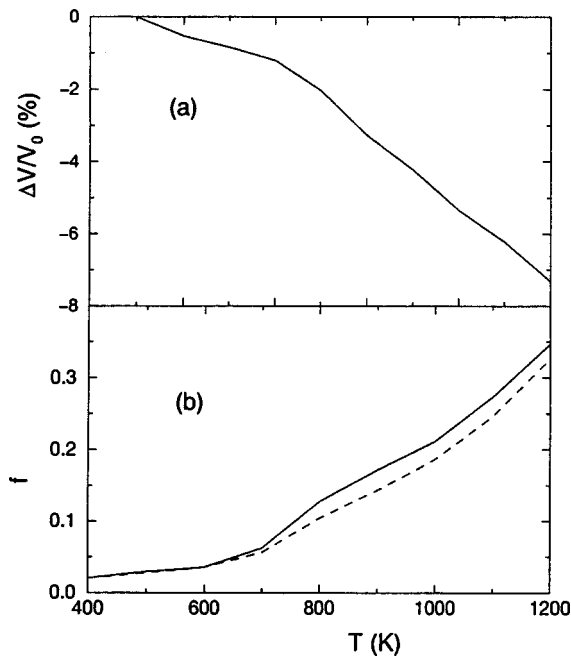


FIG. 7. Relative volume decrease (a) and the number of newly formed bonds (solid line) and broken bonds (dashed line) (b) as a function of temperature.

V. EFFECT OF THE TEMPERATURE ON DENSIFICATION AND RELAXATION PROCESS: ORIGIN OF THE THERMALLY INDUCED DENSIFICATION

A. Rebonding processes and volume decrease

As already mentioned, the experiments show temperature-induced densification of silica glass under pressure.^{25–27} Raman spectrum of the structure quenched from high temperature looked similar to the one pressurized to a pressure as large as 40 GPa.²⁵ In order to understand the structural changes in pressurized glass on heating, we have pressurized the structure to 3.6 GPa and increased the temperature in stages up to 1200 K. Long annealing for several ns has been performed at high temperatures. We have calculated the volume change during the annealing, and found that the structure densifies, with densification saturating at about 7% at the highest temperature [see Fig. 7(a)]. This value is consistent with the values of 7–8% densification observed in recent *in situ* experiments.^{26,27} This has given us confidence that the processes described in the simulation correspond to those seen experimentally.⁴⁴

It is interesting that around 700 K there is a change of slope of volume decrease, suggesting that enhanced relaxation process takes place at that temperature. We also observe that increased rebonding starts to take place after about 700 K [see Fig. 7(b)]. Below we will argue that pressure-induced densification seen experimentally has its origin in the fast rebonding and relaxation processes identified in this simulation, and that are related to the existence of extended RUM's discussed in the previous section.

B. Floppy modes and global rebonding in 3.6 GPa structure at elevated temperature

The amplitude of RUM's can reach large values, since most of the energy cost is associated with the deformation of tetrahedra, while the structure can flex and bend with no or very little energy cost.^{33,34} The ability of tetrahedral glass structures to support RUM's and their extended character have the following implications for the origin of temperature-induced densification. In the uncompressed structure, the amplitude of the RUM motion is not large enough for the oxygen atoms to move close to a Si atom of a different tetrahedron and form a bond with that atom (at the temperature reasonably below the melting point). However, when the structure is compressed to about 3 GPa, at which point no increased coordinations appear yet, but tetrahedra move very close to each other across the rings, high temperature allows an O atom to form a bond with Si atom in a different tetrahedra. This is accompanied by breaking of the old bond and subsequent relaxation of the local surrounding that can involve several new bonds formed as well as broken ones.¹⁸ This process is irreversible and is accompanied by the appearance of increased coordinations and broadening of the rings distribution.

The important point is that the temperature-induced rebonding in the pressurized yet tetrahedral (or nearly tetrahedral) structure takes place globally, since floppy modes are extended vibrations in the structure.^{21,33,34} From Fig. 4 it appears that at about 700 K the amplitude of floppy modes becomes large enough to cause enhanced rebonding in the structure. This is consistent with the value of temperature at which volume decrease is seen experimentally.^{25–27} The values of densification of 7–8% that we observe in the simulation are in a very good agreement⁴⁴ with the values obtained in the recent *in situ* experimental studies.^{26,27} We therefore suggest that temperature-induced densification observed experimentally should be attributed to the fast kinetics of rebonding processes that we have identified.

C. Floppy modes at higher pressures and pressure window

We have simulated the effect of increasing the temperature up to 1200 K in the structures at a range of pressures. We have found volume decrease similar to that shown in Fig. 7, in the structures pressurized up to 5 GPa, but not in the structures at higher pressure, although similar rebonding efficiency has been detected. We explain this effect by noting that highly pressurized structures contain enough increased coordinations to suppress the existence of the RUM's.²¹ Therefore higher temperature cannot excite large-amplitude atomic motion and cause rebonding events globally, having the effect of promoting relaxations around defects introduced by high pressure. Since temperature-induced rebonding in highly pressurized structure occurs locally, it does not result in a noticeable volume decrease.

We have seen that temperature-induced large structural changes in silica glass take place in the pressure window between about 3 and 5 GPa, the same pressure window discussed in the previous section. In this window the structure is both compact enough for the rebonding processes to take

place at high temperature (before the melting point) and RUM floppy which allows for the large-amplitude motions to take place globally in the structure.

This picture is consistent with the recent observation that the compressibility anomaly takes place earlier if the sample is pressurized at higher temperature.¹⁹ As discussed above, the right boundary of the pressure window is defined by the point at which the structure becomes unable to compress by RUM-type distortions, causing the breakdown in the medium range, and depends on the degree of stiffness due to densification and appearance of increased coordinations. Since higher temperature increases the degree of densification,^{18,19} the point at which the structure becomes stiff against RUM-type distortions is expected to take place at lower pressure, and this is what observed experimentally.

We note that the specified boundaries of pressure window were estimated using long annealing at 1200 K. The window boundaries are expected to depend on the annealing temperature, since higher temperature promotes densification and hence the rigidity of the structure. This will be studied in more detail and results will be reported elsewhere.

D. Analysis of the densified quenched structure

The temperature-induced densification at 3.6 GPa should be reflected in the densification of the quenched sample. The structure annealed for 15 ns at 3.6 GPa and 1200 K was quenched to room temperature and zero pressure and annealed for 1 ns. The quenched structure was found to be about 20% denser than original uncompressed structure, comparing well with the values reported in Ref. 25. Further annealing of the quenched structure at room temperature did not significantly affect the volume and degree of rebonding. We relate the irreversible densification of the quenched structure to rebonding and relaxation processes that result in the irreversible changes in structure on decompression.¹⁸ The comparison between initial and quenched structure shows that the degree of rebonding is significant, namely, there are 27% of newly formed bonds and 26% of broken ones.

As noted above, the Raman spectrum of the structure quenched from 3.6 GPa and high temperature was found to be similar to the one decompressed from high pressure of 40 GPa,²⁵ indicating that large structural modifications in the medium range structure have occurred. This prompted authors to suggest that at high temperature the first order transition in the dense phase has taken place. In our picture the thermally induced densification originates from the fast kinetics of rebonding processes in the pressure window, and it is interesting to analyze the modifications of the structure in the medium range that lead to the densification in the quenched sample.

We compare partial radial distribution functions $d(r) = r[g(r) - 1]$, calculated for the ideal glass configuration, glass quenched from annealing at 3.6 GPa and 1200 K, and glass quenched from 20 GPa at room temperature, in Fig. 8. The comparison shows that the structure quenched from 3.6 GPa and high temperature is very similar to the one decompressed from high pressure in the medium range. The simi-

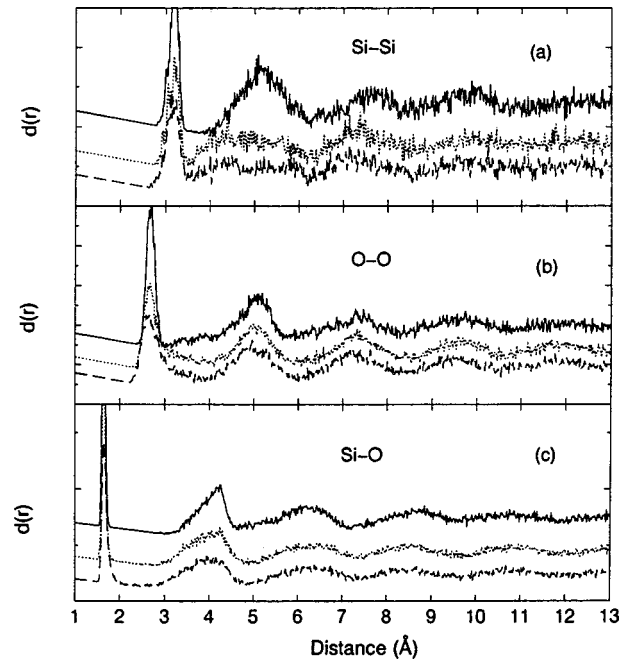


FIG. 8. $d(r)$ radial distribution function $d(r)$ calculated for ideal structure (top graphs, solid line), structure quenched from 3.6 GPa and high temperature (medium graphs, dotted line) and structure quenched from 20 GPa (lower graphs, long dashed line). Si-Si, O-O, and Si-O $d(r)$ are shown in (a), (b), and (c), respectively.

ilarity in the medium range may be related to the similarity of the Raman signal seen in Ref. 25, although we cannot speculate in more detail at this point. At the same time, the two structures differ from the ideal glass in the medium range, mostly seen in the flattening of the second Si-Si peak (see Fig. 8). We attribute this difference to the breakdown in the structure of the rings as a result of thermally induced rebonding events described above. These events take place across the rings of SiO_n tetrahedra, destroying the medium-range structure due to their irreversibility.¹⁸

It has been found that amorphous structures with different ring distributions can yield rather similar radial distribution functions.⁴⁵ Therefore the distribution of rings in the quenched structures has been calculated, using a recently developed ring search algorithm.⁴⁶ The comparison of this distribution calculated for the original and quenched structure has shown its broadening and widening (see Fig. 9). This is consistent with the previous study, in which densification of amorphous structure was related to the appearance of both smaller and larger rings.⁴⁷ We observe that the center of ring distribution in the quenched structure shifts to larger rings, with a dominance of newly appeared larger rings over smaller ones.

We find that the densified quenched structure contains about 5% Si atoms with increased number of O nearest neighbors. This number is lower than in the structure that has the same density and which is prepared by quench from high pressure at room temperature. It appears that there are two different ways to prepare densified structure that may have

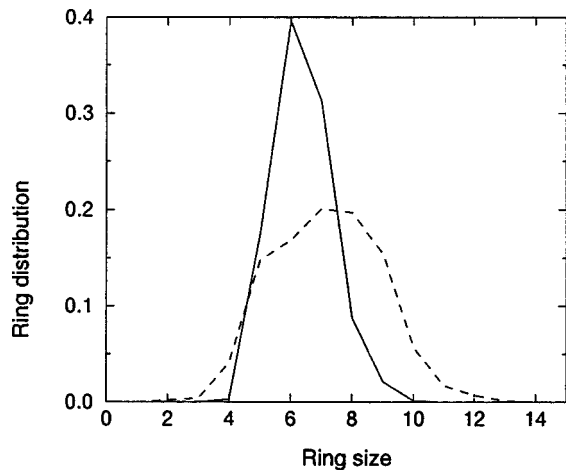


FIG. 9. Ring distribution in the ideal glass structure (solid line) and the structure quenched from 3.6 GPa after long annealing at high temperature (dashed line).

the same density but quite different topology in terms of the number of increased coordinations and rings distribution. In our earlier work we have observed *pressure-induced* rebonding events and subsequent relaxation of the structure, accompanied by the appearance of increased local coordinations.¹⁸ Here we observe yet another way to obtain a dense structure of silica glass, by causing *thermally induced* rebonding events in the structure compressed to about 3 GPa and taken to high temperature. Since the pressure is relatively low, not many increased coordinations appear in the structure, but a similar degree of densification can be achieved due to the global nature of thermally induced rebonding events.

E. Microscopic processes of relaxation to a denser phase

We have seen that higher temperature increases the kinetics of equilibration of the glass structure pressurized to 3.6 GPa, by promoting rebonding events and relaxation. It is interesting to identify the microscopic processes involved in the relaxation. In Figs. 10(a)–10(d) we plot snapshots of the ideal, pressurized, annealed and quenched structures, respectively. The highlighted atoms in all structures are the same. By comparing structures shown in Figs. 10(b) and 10(c) we find that heating up to 1200 K and long annealing for 15 ns has resulted in large displacements of some atoms. The arrow in Fig. 10 points to the chain of atoms that moved about 5 Å from initial configuration to form the threefold ring in the quenched sample. This has occurred as a result of a number of thermally induced rebonding events with subsequent relaxations in the surrounding structure.¹⁸ The interesting feature from this analysis is the cooperative nature of relaxations and large value of atomic displacements. Patches of glass appear to “flow,” as the structure equilibrates in response to external pressure and temperature through the multiple rebonding processes and subsequent relaxations.

VI. CONCLUSIONS

In summary, we have tried to shed some light into the current controversy regarding the phase transformation in

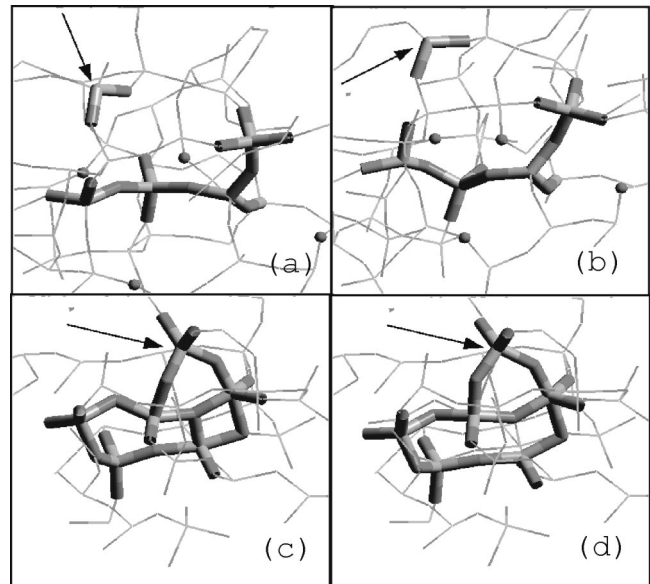


FIG. 10. Local structures of silica glass showing (a) ideal silica glass, (b) pressurized to 3.6 GPa, (c) annealed to 1200 K for 15 ns, and (d) quenched to room temperature and zero pressure. Si and O atoms are shown in grey and dark colours, respectively. Highlighted in each snapshot are the same atoms, that form the configuration with reduced number of member rings and increased configurations in (c) and (d). Arrow points to the atoms that cooperatively “flow” to close the ring in snapshot (d), moving for about 4 Å between snapshots (a) and (d).

silica glass, and into microscopic processes that accompany negative thermal swelling of pressurized glass.^{17,22,23,25,19} We have seen that the thermodynamic analysis that hints to the existence of the first-order transition around 3 GPa, is related to the existence of the threshold pressure that separates tetrahedral and nontetrahedral network. However this is not a true first-order phase transition that takes place globally in the structure and separates two distinct equilibrium phases. We have proposed the existence of pressure window between 3 and 5 GPa in which pressure distorts the structure, reducing the number of RUM’s and hence the number of ways in which the structure can distort, but without causing considerable rebonding. After 5 GPa, at which point the structure is essentially rigid, further compression causes extensive rebonding, leading to large medium-range structural modification, which is reflected experimentally in the change of volume-pressure curve and softening of the bulk modulus after about 5 GPa.¹⁹

We attribute volume decrease of the pressurized glass seen in Refs. 25–27 to the fast kinetics of rebonding and relaxation processes. We have seen that in the pressurized structure higher temperature activates rebonding between different tetrahedra across the rings. Such a rebonding takes place globally since tetrahedral (or nearly tetrahedral) glass structure is flexible against floppy modes that give rise to the large-amplitude atomic displacements. The values of densification we find in the simulation are in a very good agreement with recent experiments,^{26,27} which has allowed us to suggest that rebonding and relaxation processes are behind

the temperature-induced densification observed experimentally.

It follows from the simulation that volume decrease on temperature should take place in the pressure window between about 3 and 5 GPa. The annealing temperature is expected to affect the boundaries of the pressure window, and temperature effects will be reported separately. The challenge now is to sample the range of pressures between about 3 and 5 GPa at various temperatures, to confirm the existence of the pressure window.

We have seen that the densified quenched structure shows broadening of rings distribution, and we have identified the microscopic processes that accompany the breakdown of the medium-range structure. In particular, the interesting finding from this work has been the observation of the “flow” of the patches of silica glass structure in the form of large cooperative atomic displacements. This takes place in the process of continuous equilibration of glass through rebonding events and relaxation processes.

That silica glass is a tetrahedral network consisting of rigid units has been shown here to be important for the character and kinetics of rebonding and relaxation processes that accompany densification (flexibility against RUM motions in

particular). We may expect similar temperature-induced densification^{25–27} to take place in chemically different but structurally alike tetrahedral glasses such as GeO₂ and GeSe₂. The densification processes in GeO₂ (Ref. 17) and GeSe₂ (Ref. 4) are similar to that in silica glass, and it is plausible that temperature-induced densification of considerable magnitude can be seen in those glasses, similar to that found in silica. This makes it the subject of future experiments. As far as the nature of transition on pressure is concerned, a *diatomic* structure of these glasses appears to be related to the gradual character of transition. This is in contrast to the first-order phase transition seen in *monoatomic* amorphous Si and Ge.

ACKNOWLEDGMENTS

We are grateful to the EPSRC (UK) and Darwin College, Cambridge, for support. We are grateful to Professor V. V. Brazhkin and Professor Y. Katayama for useful discussions and for sharing the unpublished results of their recent *in situ* experiments. We thank Dr Yuan for calculating the ring distributions of the densified structures. We also thank Stephen Wells for performing the misfit analysis of RUM motion.

-
- ¹O. Mishima, J. Chem. Phys. **100**, 5910 (1994).
²O. Shimomura, S. Minomura, N. Sakai, K. Asami, K. Tamura, K. Fukushima, and H. Enod, Philos. Mag. **29**, 547 (1974).
³S. K. Deb, M. Wilding, M. Somayazulu, and P. F. McMillan, Nature (London) **414**, 528 (2001).
⁴M. Durandurdu and D. A. Drabold, Phys. Rev. B **64**, 014101 (2001).
⁵J. D. Mackenzie, J. Am. Ceram. Soc. **46**, 461 (1963).
⁶M. Grimsditch, Phys. Rev. Lett. **52**, 2379 (1984).
⁷R. J. Hemley, H. K. Mao, P. M. Bell, and B. O. Mysen, Phys. Rev. Lett. **57**, 747 (1986).
⁸A. Polian and M. Grimsditch, Phys. Rev. B **41**, 6086 (1990).
⁹S. Susman, K. J. Volin, D. L. Price, M. Grimsditch, J. P. Rino, R. K. Kalia, P. Vashishta, G. Gwanmesia, and R. C. Liebermann, Phys. Rev. B **43**, 1194 (1991).
¹⁰J. S. Tse, D. D. Klug, and Y. L. Page, Phys. Rev. B **46**, 5933 (1992).
¹¹W. Jin, R. K. Kalia, P. Vashishta, and J. P. Rino, Phys. Rev. Lett. **71**, 3146 (1993).
¹²Q. Williams and R. Jeanloz, Science **239**, 902 (1998).
¹³C. Meade, R. J. Hemley, and H. K. Mao, Phys. Rev. Lett. **69**, 1387 (1992).
¹⁴W. Jin, R. K. Kalia, P. Vashishta, and J. P. Rino Phys. Rev. B **50**, 118 (1994).
¹⁵C. S. Zha, R. J. Hemley, H. K. Mao, T. S. Duffy, and C. Meade, Phys. Rev. B **50**, 13 105 (1994).
¹⁶R. G. Della Valle and E. Venuti, Phys. Rev. B **54**, 3809 (1996).
¹⁷O. B. Tsiok, V. V. Brazhkin, A. G. Lyapin, and L. G. Khvostantsev, Phys. Rev. Lett. **80**, 999 (1998).
¹⁸K. Trachenko and M. T. Dove, J. Phys.: Condens. Matter **14**, 7449 (2002).
¹⁹F. S. El'kin, V. V. Brazhkin, L. G. Khvostantsev, O. B. Tsiok, and A. G. Lyapin, JETP Lett. **75**, 342 (2002).
²⁰M. Durandurdu and D. A. Drabold, Phys. Rev. B **65**, 104208 (2002).
²¹K. Trachenko and M. T. Dove, J. Phys.: Condens. Matter **14**, 1143 (2002).
²²D. J. Lacks, Phys. Rev. Lett. **84**, 4629 (2000).
²³E. A. Jagla, Phys. Rev. Lett. **86**, 3206 (2001).
²⁴E. A. Jagla, Phys. Rev. E **63**, 061509 (2001).
²⁵G. D. Mukherjee, S. N. Vaidya, and V. Sugandhi, Phys. Rev. Lett. **87**, 195501 (2001).
²⁶V. V. Brazhkin (private communication).
²⁷Y. Katayama (private communication).
²⁸D. Selvanathan, W. J. Bresser, P. Boolchand, and B. Goodman, Solid State Commun. **111**, 619 (1999).
²⁹J. C. Phillips, Phys. Rev. Lett. **88**, 216401 (2002).
³⁰A. J. Rader, B. M. Hespeneide, L. A. Kuhn, and M. F. Thorpe, Proc. Natl. Acad. Sci. U.S.A. **99**, 3540 (2002); D. J. Jacobs, A. J. Rader, L. A. Kuhn, and M. F. Thorpe, Proteins: Struct., Funct., Genet. **44**, 150165 (2001); M. F. Thorpe, M. Lei, A. J. Rader, D. J. Jacobs, and L. A. Kuhn, J. Mol. Graphics **19**, 60 (2001).
³¹W. Smith and T. Forester, J. Mol. Graphics **14**, 136 (1996).
³²F. Wooten, K. Winer, and D. Weaire, Phys. Rev. Lett. **54**, 1392 (1985); F. Wooten and D. Weaire, Phys. Rev. Lett. **40**, 1 (1987).
³³K. Trachenko, M. T. Dove, K. Hammonds, M. Harris, and V. Heine, Phys. Rev. Lett. **81**, 3431 (1998).
³⁴K. Trachenko, M. T. Dove, M. Harris, and V. Heine, J. Phys.: Condens. Matter **12**, 8041 (2000).
³⁵K. Trachenko, M. T. Dove, and V. Heine, Phys. Rev. B **65**, 092201 (2002).
³⁶S. Tsuneyuki, M. Tsukada, H. Aoki, and Y. Matsui, Phys. Rev. Lett. **61**, 869 (1998).

- ³⁷S. Tsuneyuki, Y. Matsui, H. Aoki, and M. Tsukada, *Nature* (London) **339**, 209 (1989).
- ³⁸D. J. Lacks, *Phys. Rev. Lett.* **80**, 5385 (1998).
- ³⁹K. Mizushima, S. Yip, and E. Kaxiras, *Phys. Rev. B* **50**, 14 952 (1994).
- ⁴⁰M. T. Dove, *Introduction to Lattice Dynamics* (Cambridge University Press, Cambridge, 1993).
- ⁴¹I. Saika-Voivod, F. Sciortino, and P. H. Poole, *Phys. Rev. E* **63**, 011202 (2000).
- ⁴²M. F. Thorpe, *J. Non-Cryst. Solids* **57**, 355 (1983); M. F. Thorpe, B. R. Djordjevic, and D. J. Jacobs, in *Amorphous Insulators and Semiconductors*, edited by M. F. Thorpe and M. I. Mitkova (Kluwer, Dordrecht, 1997), Vol. 289.
- ⁴³S. A. Wells, M. T. Dove, M. G. Tucker, and K. Trachenko, *J. Phys.: Condens. Matter* **14**, 4645 (2002).
- ⁴⁴The value of temperature-induced densification was reported to be 20% at 3.6 GPa in Ref. 25. This is different from the values found in other *in situ* experiments (Refs. 26,27). We note that, in addition to 20% thermally induced densification at high pressure, Ref. 25 also reported a similar degree of densification of the sample quenched to zero pressure and room temperature. Since these two observations are difficult to reconcile, we feel this work is not unambiguous regarding the values of densification.
- ⁴⁵X. Yuan, M. Pulim, and L. W. Hobbs, *J. Nucl. Mater.* **289**, 71 (2001).
- ⁴⁶X. Yuan and A. N. Cormack, *Comput. Mater. Sci.* **24**, 343 (2002).
- ⁴⁷L. W. Hobbs, C. E. Jesurum, V. Pulim, and B. Berger, *Philos. Mag.* **78**, 679 (1998).